Al-Azhar University Civil Engineering Research Magazine (CERM)
Vol. (41) No. (1) January, 2019

The Effect of Ionosphere on GPS observations

Ahmed Elsayed[1], Ahmed Sedeek[2], Mohamed Doma[3], Ahmed Elgohary[4]

1. Faculty of Engineering, Menofia University, Egypt,
2. Doctor at Higher Institute of Engineering and Technology, El-Behira, Egypt,
3. Associate Professor at Faculty of Engineering, Menofia University, Egypt,
4. Doctor at Faculty of Engineering, Menofia University, Egypt.

الملخص العربي

إن طبقة الأيونوسفير مرتبطة بشكل كبير بنظام تحديد المواقع العالمي حيث أنها تعتبر من أكبر مصادر الأخطاء التي لابد أن يتم التخلص منها للحصول على إحداثيات دقيقة. فهذه الطبقة تسبب إنكسار وإنحراف لإشارة القمر الصناعي مما يسبب تأخر في هذه الإشارة قبل وصولها لجهاز الإستقبال مما يسبب زيادة في زمن إنتقال الإشارة مما ينتج عنه خطأ في تعيين الإحداثيات. نتيجة خاصية الإنتشارية التي تتميز بها طبقة الأيونوسفير فإنه من الممكن حساب قيمة هذا الخطأ بإستخدام أجهزة إستقبال لها القدرة على إستقبال ترددين على الأقل. الهدف الأساسي من هذا البحث الحالي هو حساب تأثير طبقة الأيونوسفير بدقة على أرصاد نظام تحديد المواقع العالمي من خلال إستخدام جهاز إستقبال لديه القدرة على إستقبال أكثر من إشارة من نفس القمر الصناعي في نفس الوقت. يستخدم النموذج الرياضي المستخدم في هذا البحث قياسات فرق الطور بدلاً من قياسات الشفرة للحصول على دقة أكبر في حساب الخطأ الناتج عن تأثير الأيونوسفير على إشارة القمر الصناعي. يفترض النموذج الرياضي المستخدم في هذا البحث أن تأثير طبقة الأيونوسفير يتركز على إرتفاع ثابت عادة ما يؤخذ 350 كم. يعتمد هذا النموذج الرياضي المستخدم على العدد الصحيح للموجات المنتقلة من القمر الصناعي لجهاز الإستقبال وكذلك قيمة إحداثيات نقطة تقاطع الخط الواصل بين القمر الصناعي وجهاز الإستقبال مع موضع تمركز تأثير طبقة الأيونوسفير. تم إستخدام برنامج الماتلاب لكتابة هذا النموذج الرياضي وتم تطبيقه على ثمانية محطات موزعين على أماكن مختلفه على سطح الأرض. لتقييم هذا النموذج الرياضي تم مقارنة نتائج تأثير الأيونوسفير على إشارات الأقمار الصناعية الناتجة من هذا النموذج مع برنامج تحليل وتحديد المواقع.

Abstract

The ionosphere is significantly related to GPS and the refraction it causes in GPS signal is considered one of the main sources of errors which must be eliminated to determine accurate positions. An apparent delay is occurred in GPS signal due to both refraction and diffraction caused by the atmosphere. The second region of the atmosphere is the ionosphere. GPS receiver networks have been used for monitoring the ionosphere for a long time. The ionospheric delay is the most predominant of all the error sources. This delay is a function of the total electron content (TEC). Because of the dispersive nature of the ionosphere, one can estimate the ionospheric delay using the dual frequency GPS measurements. In the current research our primary goal is applying Precise Point Positioning (PPP) observation for accurate ionosphere error modeling, by estimating Ionosphere delay using carrier phase observations from dual frequency GPS receiver. The proposed algorithm was written using MATLAB. The proposed Algorithm depends on the geometry-free carrier-phase observations after detecting cycle slip to estimates the ionospheric delay using a spherical ionospheric shell model, in which the vertical delays are described by means of a zenith delay at the station position and latitudinal and longitudinal gradients. Geometry-free carrier-phase observations were applied to avoid unwanted effects of pseudo-range measurements, such as code multipath. The ionospheric estimation in this algorithm is performed by means of sequential least-squares adjustment. Finally, an adaptable user interface MATLAB software are capable of estimating ionosphere delay, ambiguity term and ionosphere gradient accurately.

Key words: GPS, Ionosphere delay, PPP.

1. Introduction

During the transmission of GPS signals from satellite to receiver, the signals propagate through the ionosphere so that the ionospheric delay is closely associated with GPS and is considered one of the main sources of errors in point positioning using GPS techniques, on the other hand GPS can be used as a sensor of the ionosphere and investigate its characteristics because of the global system coverage and the availability of multiple frequency data. In this paper we used GPS receiver as a sensor of the ionosphere. The ionosphere is a dispersive medium, which means that the delay depends on the frequency of the signal. the first order effect of the ionosphere refraction could be eliminated mathematically by means of a linear combination of the signals on the two frequencies, because GPS signals are broadcast on more than one frequency. This combination is widely called the iono-free combination (Leandro, 2009).

Various methods were devised to calculate the ionospheric delay. These methods were based on spherical harmonic expansions in the global or regional scale (e.g. Schaer, 1999, and Wielgosz et al., 2003a). Local methods were based on two-dimensional Taylor series expansions (e.g. Komjathy, 1997, Jakobsen et al., 2010, Deng et al., 2009, and Masaharu et al., 2013).

This paper is aimed to apply Precise Point Positioning (PPP) observation for accurate ionosphere error modeling, using carrier phase measurements the proposed algorithm was written using MATLAB.

2. Observations equations for carrier measurements.

The observations of dual-frequency GPS receiver at any station consists of two codes and two carrier phase observations in RINEX format which were used for present model. The observations equations for carrier-phase measurements are used in this study because they are more accurate than code measurements and can be formulated as follows (Leandro, 2009; Sedeek et al., 2017):

$$\Phi = R + c(dt - dT) + T - I + \lambda N + pb_r - pb_s + hd_r - hd_s + m + e \quad (1)$$

Where Φ, R, C, dT and dt, T, I, γ, N , λ , hdr and hds , pbr and pbs and m are the carrier-

Phase measurements, in meter, the geometric distance between satellite and receiver antennas, in meters, the speed of light, in meters per second, the receiver and satellite clock errors, respectively, in seconds, the neutral troposphere delay, in meters, the ionosphere delay, in meters, the carrier-phase integer ambiguity, the carrier-phase wave length, in meters, the receiver and satellite carrier-phase hardware delays, respectively, in metric units, the receiver and satellite carrier-phase initial phase bias, respectively, in metric units, the carrier-phase multipath, in meters, respectively and e is the un-modeled errors of carrier-phase measurements, in meters.

3. Estimation of Ionospheric Delay by Geometry-Free Combination of GPS Observables.

The geometry-free linear combination of GPS observations is classically used for ionospheric investigations. It can be obtained by subtracting simultaneous pseudo range (P1-P2 or C1-P2) or carrier phase observations (Φ1-Φ2). With this combination, the satellite – receiver geometrical range and all frequency independent biases are removed

(Ciraolo et al., 2007). The ionospheric estimation is performed using the following model (Leandro, 2009):

$$\phi_{GF} = \phi_{L1} - \phi_{L2} = (1-\gamma)\mathrm{MF}\left(I_{v,0} + \nabla_{\phi}(\phi_P - \phi_0) + \nabla_{\lambda}(\lambda_P - \lambda_0)\right) + Nb'_{gf} \tag{2}$$

where ϕ_{GF} is the geometry-free carrier-phase observation in length units, MF is the ionosphere mapping function, $I_{v,0}$ is the vertical ionospheric delay at the station position, $\nabla\varphi$ and $\nabla\lambda$ are latitudinal and longitudinal gradients, respectively, ϕ_P and λ_P are the geodetic latitude and longitude of the ionospheric piercing point, ϕ_0 and λ_0 are the geodetic latitude and longitude of the station, γ *is the* factor to convert the ionospheric delay from L1 to L2 frequency, unitless and Nb'_{gf} is an ambiguity parameter which includes the carrier-phase integer ambiguity plus a collection of biases. The mapping function is based on a spherical ionospheric shell model as shown in Figure 1, and is computed according to (Leandro, 2009):

$$\mathrm{MF} = \sqrt{1 - \left(\left(\frac{r}{(r+sh)}\right)\cos(e)\right)^2} \tag{3}$$

Where r is the mean radius of earth,sh is the ionospheric shell height (default value is 350 km), e is the satellite elevation angle at the shell height piercing point, and e is the elevation angle of satellite S as seen from station O.

To compute elevation and azimuth angle for any satellite (e , $Azim$), the receiver position in Earth Centered Earth Fixed (ECEF) is converted to geodetic coordinates (λ, φ, z). Then, the satellite position coordinate (x_s , y_s , z_s) from ECEF at the specified epoch is interpolated from the IGS final orbits.

The interpolated satellite position is then transformed to a local coordinate frame, East, North, and Up (ENU) system. The transferred ENU is used to calculate elevation and azimuth angles as follows (Dahiraj, 2013 and Sedeek et al, 2017):

$$e = tan^{-1}\left(\frac{x_U}{\sqrt{x_N^2 + x_E^2}}\right) \tag{4}$$

$$Azim = tan^{-1}\left(\frac{x_E}{x_N}\right) \tag{5}$$

Usually, the ionosphere is assumed to be concentrated on a spherical shell located at altitude (nominally taken as 350 km above Earth's surface. Ionospheric Pierce Point is the intersection point between the satellite receiver line-of-sight, and the ionosphere shell as shown in Figure (1).

IPP location can be computed by providing reference station coordinate (Φ_0 , λ_0), then the geographic latitude and longitude of IPP can be computed according to elevation and azimuth angle of satellite (Dahiraj, 2013). The offset angel between the IPP and the receiver (Ψ) is defined as the offset between the IPP and the user's receiver. The elevation angle (β) the offset angel between the IPP and the receiver (Ψ) are computed as follow (El Gizawy,2003):

$$\beta = cos^{-1}\left(\left(\frac{r}{(r+sh)}\right)\cos(e)\right) \tag{6}$$

$$\Psi = \beta - \mathrm{e} = cos^{-1}\left(\left(\frac{r}{(r+sh)}\right)\cos(e)\right) - e \tag{7}$$

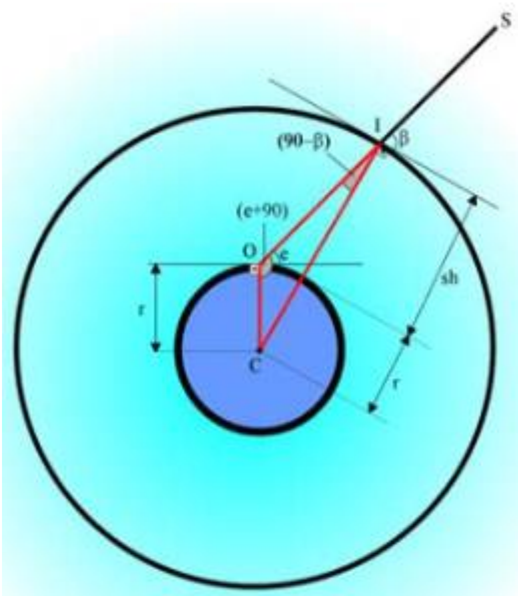

Figure (1). Elements of the ionospheric shell model (Leandro, 2009).

Where r and sh are the mean radius of the spherical Earth and the height of IPP, respectively. Given the user's receiver coordinates (ϕ_0 , λ_0), and the offset angle Ψ , the pierce point coordinates ($\phi_{IPP}, \lambda_{IPP}$) are then derived by the following expressions (El-Gizawy, 2003):

$$\phi_{IPP} = (\phi_r + \Psi \cos(\text{Azim})) \quad (8)$$

$$\lambda_{IPP} = \left(\lambda_r + \frac{\Psi\, sin(Azim)}{cos(\phi_{IPP})}\right) \quad (9)$$

The ionospheric estimation is performed by means of sequential least-squares adjustment, where the parameters are the ionospheric model elements (vertical delay and gradients) and the ambiguities as follows:

$$L = A\,X \quad (10)$$

Where: L is the vector of observations, A is the design matrix, X is unknown parameters vector, and P is weight matrix of observations.

$$X = (A_1^T.P_1.A_1 + A_2^T.P_2.A_2)^{-1}(A_1^T.P_1.L_1 + A_2^T.P_2.L_2) \quad (11)$$

By using this system of equations, vertical ionospheric delay, latitudinal and longitudinal gradients values at the station position are computed on an epoch by epoch basis.

4. Results and Discussions

In the present contribution, eight IGS stations were used to evaluate the performance of the proposed model. The geographic Longitude and Latitude of these stations are shown in table (1):

Table (1): - The geographic Longitude and Latitude of IGS stations which were used in this study.

	Geodetic Coordinates			Geodetic Coordinates	
Station	**Longitude**	**Latitude**	**Station**	**Longitude**	**Latitude**
CEBER	-4.3679 °	40.4534 °	**MADR**	-4.2497 °	40.4292 °
FRDN	-66.6599 °	45.9335 °	**MAT1**	16.7045 °	40.6491 °
HERS	50.8673°	0.3363°	**METS**	24.3953 °	60.2175 °
HUEG	7.5962 °	47.8340 °	**NRC1**	- 75.6238 °	45.4542 °

The Ionosphere delay is estimated for observations of DOY 3, 2018 for these eight stations and the results were compared with the results of the online version of the GPS Analysis and Positioning Software (GAPS) as shown in the following figures, and the average ionospheric delay of each station using the Proposed code and GAPS is shown in table (2).

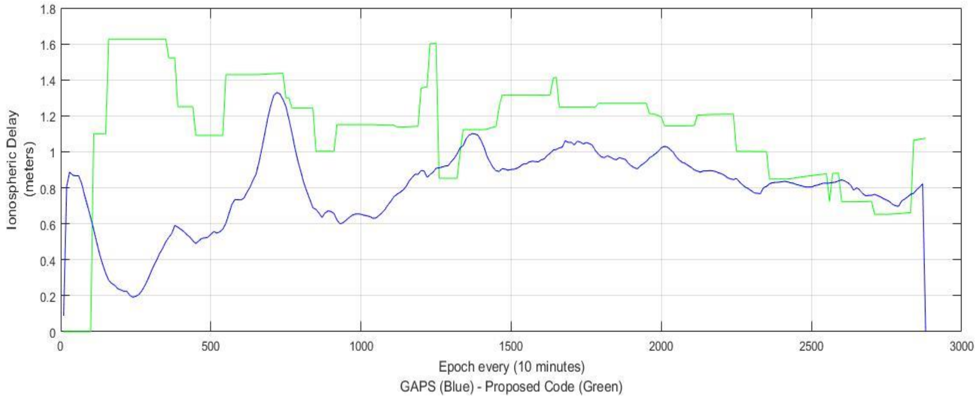

Figure (2). Vertical Ionosphere delay of CEBER station estimated by the proposed code and GAPS of DOY 3, 2018.

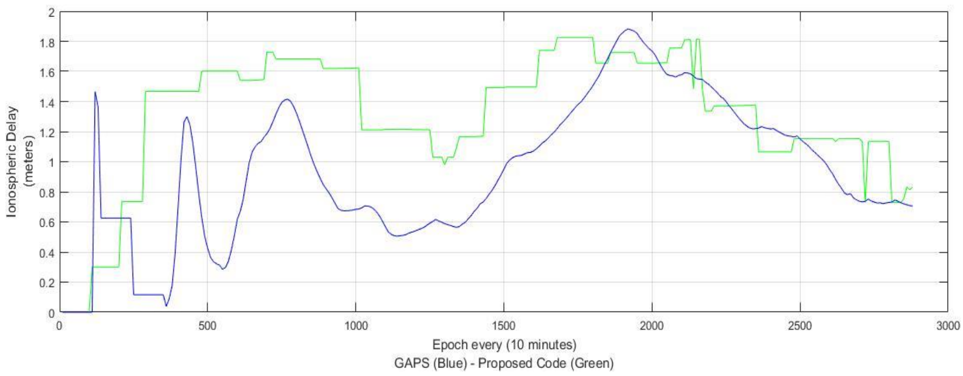

Figure (3). Vertical Ionosphere delay of FRDN station estimated by the proposed code and GAPS of DOY 3, 2018.

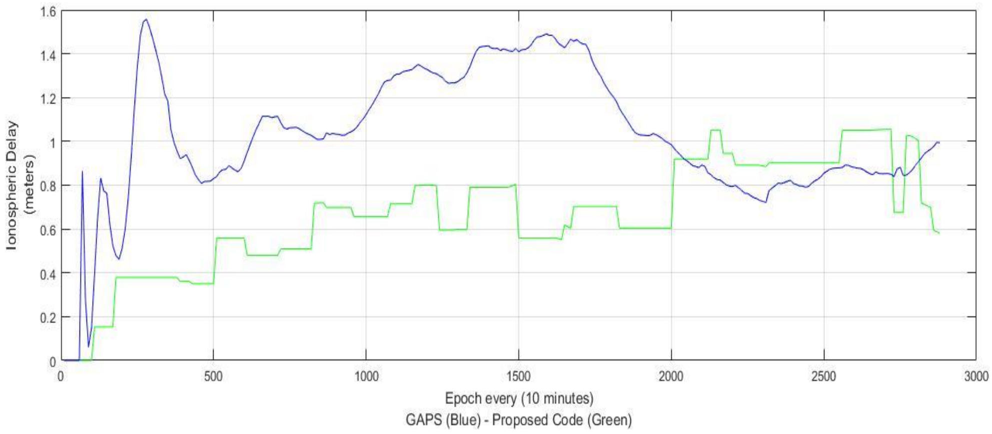

Figure (4). Vertical Ionosphere delay of HERS station estimated by the proposed code and GAPS of DOY 3, 2018.

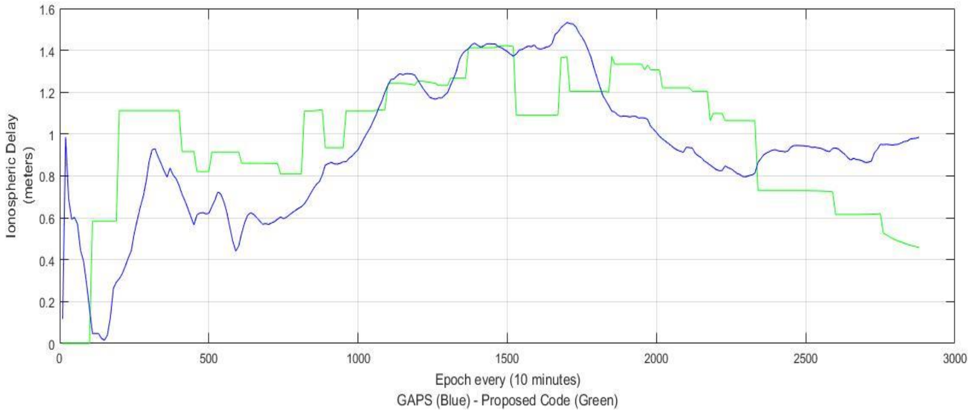

Figure (5). Vertical Ionosphere delay of HUEG station estimated by the proposed code and GAPS of DOY 3, 2018.

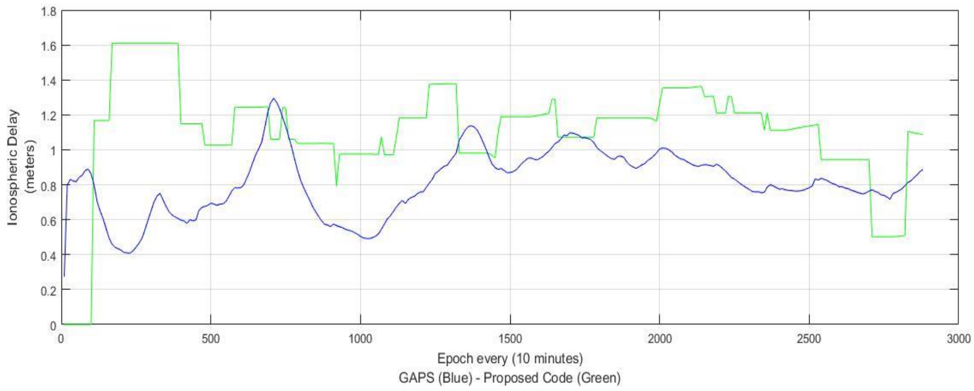

Figure (6). Vertical Ionosphere delay of MADR station estimated by the proposed code and GAPS of DOY 3, 2018.

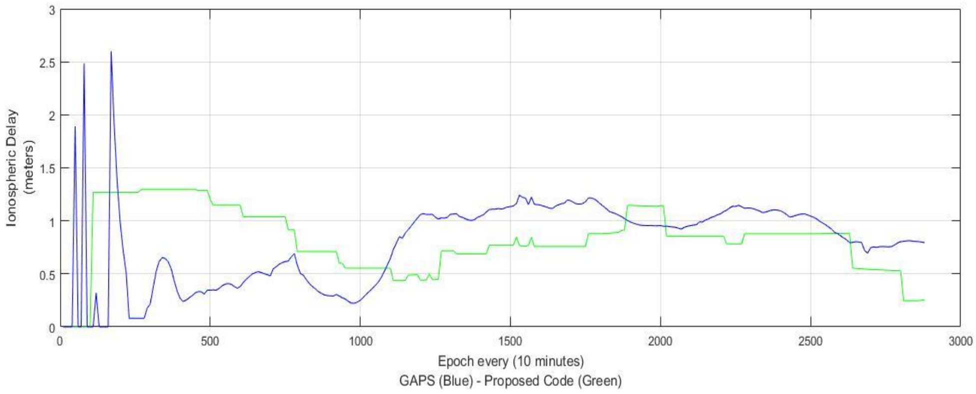

Figure (7). Vertical Ionosphere delay of MAT1 station estimated by the proposed code and GAPS of DOY 3, 2018.

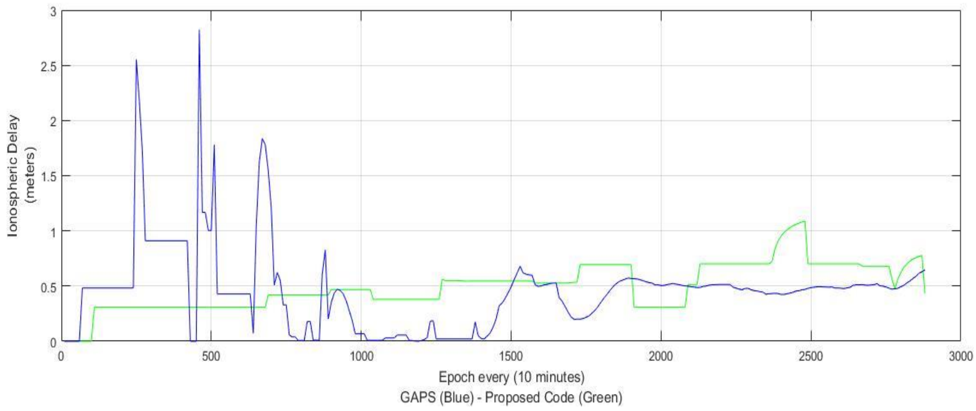

Figure (8). Vertical Ionosphere delay of METS station estimated by the proposed code and GAPS of DOY 3, 2018.

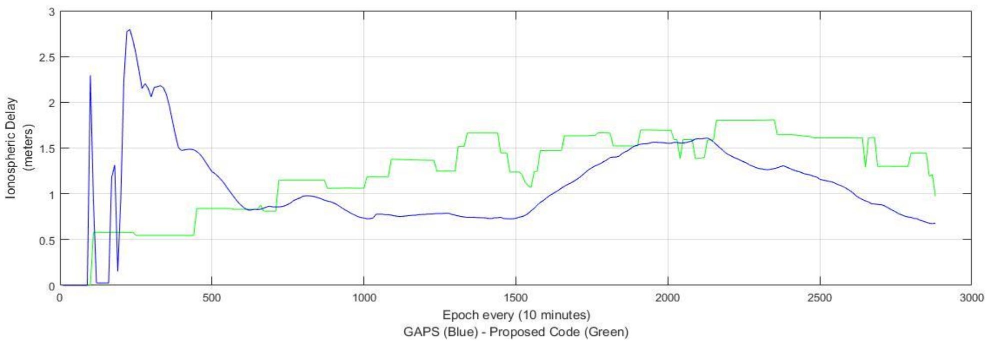

Figure (9). Vertical Ionosphere delay of NRC1 station estimated by the proposed code and GAPS of DOY 3, 2018.

Previous figures show a comparison of the ionospheric delays computed with the proposed code and GAPS.

Table (2): - The average Ionospheric Delay of each station of DOY 3, 2018 using the Proposed code and GAPS.

	Average Ionospheric Delay (m)			Average Ionospheric Delay (m)	
Station	**Proposed Code**	**GAPS**	**Station**	**Proposed Code**	**GAPS**
CEBER	1.1203	0.7948	**MADR**	1.6838	0.8126
FRDN	1.3139	0.9387	**MAT1**	0.8189	0.9771
HERS	0.6594	1.0255	**METS**	0.4961	0.5106
HUEG	0.9790	0.9328	**NRC1**	1.2463	1.0848

This comparison shows how much the accuracy of this study is good in terms of agreement of solutions provided by GAPS.

5.CONCLUSIONS

We have overviewed an algorithm which can be used to estimate ionospheric delays of GPS observations using single GPS receiver using a spherical ionospheric shell model. This Algorithm depends on the geometry-free carrier-phase observations after detecting cycle slip. The ionospheric estimation in this algorithm is performed by means of Sequential least-squares adjustment. This study is performed on eight IGS stations. Previous figures and table (2) show an agreement of the proposed code results and values provided by GAPS. This procedure may be better than GAPS because it can estimate the ionospheric delays each thirty seconds whereas GAPS estimate the ionospheric delays each ten minutes.

6. References:

Ciraolo, L., Azpilicueta, F., Brunini, C., Meza, A., and Radicella S., M., (2007), Calibration errors on experimental Slant Total Electron Content (TEC) determined with GPS, Journal of Geodesy, Vol. 81, No. 2, pp. 111–120.

Deng, Z., M., Bender G. Dick, Ge M., Wickert J., Ramatschi M., and Zou X. (2009), Retrieving tropospheric delays from GPS networks densified with single frequency receivers. Geophysical Research Letters, VOL. 36, L19802, doi:10.1029/2009GL040018.

Dahira jsunehra., (2013), Validation of GPS receiver instrumental bias results for precise navigation.
Indian Journal of Radio& space Physics, Vol. 42June 2013. pp.175-181.

El-Gizawy, M. L., 2003, Development of An Ionosphere Monitoring Technique Using GPS Measurements for High Latitude GPS Users. Master of Science. University of Calgary, Canada.

Guochang Xu., (2007), GPS Theory, Algorithms and Applications, Library of Congress Control Number: 2007929855. ISBN second edition 978-3-540-72714-9 Springer Berlin Heidelberg New York.

Hofmann-Wellenhof, B., Lichtenegger H., and WalseE., (2008), GNSS Globa lNavigation Satellite Systems; GPS, Glonass, Galileo & more, Springer Wien, New York.

Jakobsen J., Knudsen P., Jensen A., (2010), Analysis of local ionospheric time varying characteristics with singular value decomposition, Journal of Geodesy 85 (7) pages 449456, http://dx.doi.org/10.1007/s00190-010-0378-2.Special Issue on the 43rd ISCIE International Symposium on Stochastic.

Komjathy, A., (1997), Global Ionospheric Total Electron Content Mapping Using the Global Positioning System, Ph.D. dissertation, Department of Geodesy and Geomatics Engineering Technical Report No. 188, University of New Brunswick, Fredericton, New Brunswick, Canada, 248 p.

Leandro R. F., (2009), Precise Point Positioning with GPS: A New Approach for Positioning, Atmospheric Studies, and Signal Analysis, Ph.D. dissertation, Department of Geodesy and Geomatics Engineering, Technical Report No. 267, University of New Brunswick, Fredericton, New Brunswick, Canada, 232 pp.

Masaharu Ohashi, Taisuke Hattori, Yukihiro Kubo and Sueo Sugimoto., (2013), Multi-Layer Ionospheric VTEC Estimation for GNSS Positioning, special Issue on the 43rd ISCIE International Symposium on Stochastic Systems Theory and Its Applications-III Vol. 26, No. 1, pp. 16–24, 2013.

Sedeek A. A., Doma M. I., Rabah M. and Hamama M. A., (2017), Determination of Zero Difference GPSDifferential Code Biasesfor Satellites and Prominent Receiver Types, Arabian journal of geosciences, vol. 10, January 2017.

Schaer, S., (1999), Mapping and Predicting the Earth's Ionosphere Using the Global Positioning System, PhD dissertation, Astronomical Institute, University of Berne, Switzerland, pp. 205.

Wielgosz P., L.W. Baran, I.I. Shagimuratov and M.V. Aleshnikova., (2003a), Latitudinal variations of TEC over Europe obtained from GPS observation, accepted by Annales Geophysicae.

Wielgosz, P., Grejner- Brzezinka, D. and Kashani, I., (2003b), Regional Ionosphere Mapping with Kriking and Multiquadric Methods, Journal of Global Positioning Systems, vol. 2, no. 1, pp 48-55.